

Influence of third-body particles originating from bone void fillers on the wear of ultra-high-molecular-weight polyethylene

Raelene M Cowie¹, Silvia Carbone¹, Sean Aiken², John J Cooper² and Louise M Jennings¹

Proc IMechE Part H:
J Engineering in Medicine
2016, Vol. 230(8) 775–783
© IMechE 2016



Reprints and permissions:
sagepub.co.uk/journalsPermissions.nav
DOI: 10.1177/0954411916651461
pih.sagepub.com



Abstract

Calcium sulfate bone void fillers are increasingly being used for dead space management in infected arthroplasty revision surgery. The presence of these materials as loose beads close to the bearing surfaces of joint replacements gives the potential for them to enter the joint becoming trapped between the articulating surfaces; the resulting damage to cobalt chrome counterfaces and the subsequent wear of ultra-high-molecular-weight polyethylene is unknown. In this study, third-body damage to cobalt chrome counterfaces was simulated using particles of the calcium sulfate bone void fillers Stimulan[®] (Biocomposites Ltd., Keele, UK) and Osteoset[®] (Wright Medical Technology, TN, USA) using a bespoke rig. Scratches on the cobalt chrome plates were quantified in terms of their density and mean lip height, and the damage caused by the bone void fillers was compared to that caused by particles of SmartSet GMV PMMA bone cement (DePuy Synthes, IN, USA). The surface damage from Stimulan[®] was below the resolution of the analysis technique used; SmartSet GMV caused 0.19 scratches/mm with a mean lip height of 0.03 μm ; Osteoset[®] led to a significantly higher number (1.62 scratches/mm) of scratches with a higher mean lip height (0.04 μm). Wear tests of ultra-high-molecular-weight polyethylene were carried out in a six-station multi-axial pin on plate reciprocating rig against the damaged plates and compared to negative (highly polished) and positive control plates damaged with a diamond stylus (2 μm lip height). The wear of ultra-high-molecular-weight polyethylene was shown to be similar against the negative control plates and those damaged with third-body particles; there was a significantly higher ($p < 0.001$) rate of ultra-high-molecular-weight polyethylene wear against the positive control plates. This study showed that bone void fillers of similar composition can cause varying damage to cobalt chrome counterfaces. However, the lip heights of the scratches were not of sufficient magnitude to increase the wear of ultra-high-molecular-weight polyethylene above that of the negative controls.

Keywords

Knee replacement, third-body damage, calcium sulfate, bone void filler, wear, ultra-high-molecular-weight polyethylene, in vitro

Date received: 5 August 2015; accepted: 29 April 2016

Introduction

Over 140,000 primary arthroplasty procedures are carried out in the National Health Service (NHS) annually¹ with the aim of reducing pain and restoring joint function in patients with osteoarthritis. Despite an estimated survivorship of greater than 95% at 10 years, failure of metal-on-polyethylene implants most commonly occurs as a result of wear of the ultra-high-molecular-weight polyethylene (UHMWPE) component² leading to aseptic loosening. To reduce the potential for aseptic loosening due to wear debris-induced osteolysis, the wear of the UHMWPE component should be

minimised. Counterface roughness is one of the most important determinants of wear volumes and the number and morphology of micron and sub-micron size particles generated.^{3,4} It only requires a single hard

¹Institute of Medical and Biological Engineering, School of Mechanical Engineering, University of Leeds, Leeds, UK

²Biocomposites Ltd., Keele, UK

Corresponding author:

Louise M Jennings, Institute of Medical and Biological Engineering, School of Mechanical Engineering, University of Leeds, Leeds LS2 9JT, UK.
Email: l.m.jennings@leeds.ac.uk

particle to enter the contact surfaces to cause a single scratch of 2 μm depth to produce a large increase in UHMWPE wear³ with the wear rate primarily dependent on the scratch lip height.⁴ Damage to the cobalt chrome counterface causes a change in the dominant wear mechanism from adhesive to abrasive, which accelerates UHMWPE wear.⁵ Clinically, femoral counterfaces can be roughened by bone cement particles, bone particles, and metallic debris, which when trapped between the articulating surfaces can cause damage to the bearing surfaces and accelerate wear.⁶ The presence of third-body particles such as bone cement, bone fragments, or porous-coating beads in retrieved devices and surrounding tissue⁷ has been widely reported with the particles originating during device implantation, from the device itself, or from failure of the cement mantle.^{7,8}

There have been several approaches to experimentally recreating the damage to articulating surfaces by third-body particles in total joint replacements and subsequently determining the wear of UHMWPE. In order to generate reproducible scratches which replicate those observed on clinical retrievals, the most reliable method has been to use a diamond stylus to directly scratch the counterface surface.^{3,5,6,9,10} Other approaches have included tumbling the implant in a material such as alumina powder^{11,12} or roughening with silicone carbide paper.^{13–16} However, these approaches cannot be controlled as effectively as scratching directly with a diamond stylus. Several studies have introduced third-body particles into the lubricant used for wear testing.¹⁷ These particles have been derived from bone^{18–20} or synthetic materials such as bone cement^{8,21} or aluminium oxide particles.^{22,23} However, when dosing the lubricant, it is very difficult to control which, if any, of the particles become entrained into the articulating surfaces. The challenge is therefore to recreate clinically relevant surface damage using third-body particles, to quantify this damage using appropriate surface topographical measurements, and to determine the wear of UHMWPE.

The third-body damage method used in this study was adapted from previous work by Minakawa.²⁴ In Minakawa's study, particles of bone and bone cement were trapped between a truncated cone UHMWPE pin and flat plates composed of different materials typically used as the hard bearing material in joint arthroplasty. The pin was axially loaded using a materials testing machine, and the plate was pulled beneath the pin via a pulley system recreating third-body damage. To give the surface damage clinical relevance, the bearing materials and third-body particles were similar to those used in joint arthroplasty and the third-body particles were controlled in a size range found in retrieved implants.

In this study, however, the third-body particles used were derived from calcium sulfate bone void fillers (BVF), which are increasingly being used in revision procedures for the management of infected prostheses.²⁵ Superficial infection of total knee

replacements can often be successfully treated using systemic antibiotics while deep infection is more usually treated with debridement and washout often resulting in revision of the implant.^{26–29} Such debridement can lead to significant dead space which becomes a potential source of re-infection. To manage this dead space, a variety of materials have been considered including polymethyl methacrylate (PMMA) bone cement and resorbable materials such as hydroxyapatite, collagen, fibrin, various polymers such as polylactides, and calcium sulfate.^{30,31} Calcium sulfate BVFs provide a low-cost, synthetic alternative to allogenic bone grafts; they are biocompatible, resorbable, and osteoconductive and do not elicit a foreign body or inflammatory response.³² They resorb in approximately 6–8 weeks when implanted in a bone void^{33,34} and may be loaded with antibiotics which are slowly and locally released as the calcium sulfate resorbs.^{35,36} However, there are concerns over the potential for loose beads of BVFs to migrate into the joint space causing third-body damage and accelerating UHMWPE wear. For one material to scratch another, the hardness of the scratching material must be similar to or greater than that of the scratched material. Calcium sulfate has a lower hardness compared to materials already known to damage metal counterfaces, including barium sulfate and zirconium dioxide, which are commonly added to PMMA bone cement to improve the radiopacity,^{8,18} however, depending on the processing route, calcium sulfate BVFs can contain impurities.³⁷

The aim of this study was to determine the surface damage to cobalt chrome counterfaces if third-body particles originating from BVFs or PMMA bone cement were to become trapped between the articulating surfaces of a joint replacement. Following damage simulation, the wear performance of UHMWPE was assessed against the cobalt chrome counterfaces using a multi-axial pin on plate reciprocating rig with tribological and kinematic conditions to reflect the contact pressure and cross-shear in total knee replacements.³⁸ Due to the lower hardness of calcium sulfate compared with materials already used in joint replacement procedures such as the barium sulfate and zirconium dioxide in PMMA bone cement, it was hypothesised that if pellets of BVFs were to become trapped between the articulating surfaces of a total knee replacement there would be no influence on the wear of the UHMWPE.

Materials and methods

In accordance with the previous methodology described by Minakawa,²⁴ the study was split into two phases: the first phase comprised third-body damage to cobalt chrome counterfaces with different third-body particles; the second phase consisted of experimental wear simulation against the damaged surfaces. This approach gave greater control over the number of particles trapped between the articulating surfaces¹⁸ and is

Table 1. Components used in this study.

Components	
GUR 1020 UHMWPE pins 3 mm flat contact face (conventional, unsterilised)	
GUR 1020 UHMWPE pins 5 mm flat contact face (conventional, unsterilised)	
Cobalt chrome plates ($R_a < 0.01 \mu\text{m}$)	
UHMWPE: ultra-high-molecular-weight polyethylene.	

Table 2. Third-body particles used for damage simulation.

Third-body particles	
PGCS: Stimulan [®] bone void filler beads (3 mm), Biocomposites Ltd., Keele, UK	
MGCS: Osteoset [®] bone void filler pellets (3 mm), Wright Medical Technology, TN, USA	
PMMA: SmartSet GMV [®] Gentamicin bone cement (+ 10% barium sulfate), DePuy Synthes, IN, USA, prepared to 500–1000 μm particles	
PGCS: pharmaceutical grade calcium sulfate; MGCS: medical grade calcium sulfate; PMMA: polymethyl methacrylate.	

accepted practice to recreate damage and subsequently perform wear testing.^{3,5,10}

Materials

The components and third-body materials used are shown in Tables 1 and 2.

Third-body particles were generated from polymerised PMMA-GMV (SmartSet GMV PMMA bone cement, DePuy Synthes Joint Reconstruction, IN, USA) with 10% barium sulfate, cement particles were filtered and those in the size range of 500–1000 μm diameter were used for damage simulation; Stimulan[®] a recrystallised pharmaceutical grade of calcium sulfate—PGCS (Biocomposites Ltd, Keele, UK) and Osteoset[®] a medical grade calcium sulfate—MGCS (Wright Medical Technology, TN, USA). The brittle BVFs were crushed prior to testing.

The pins used in the damage simulation and wear testing reflected the grade of polyethylene used in total knee replacement, GUR 1020 UHMWPE³⁸ (conventional, unsterilised) and had a truncated cone geometry. Those used for damage simulation had a flat 3 mm diameter contact face and those used for wear simulation had a flat 5 mm diameter contact face. Pins used for wear simulation were soaked in sterile water for a minimum of 2 weeks prior to testing to maximise their water uptake. Highly polished (mean surface roughness, $R_a < 0.01 \mu\text{m}$) cobalt chrome (CoCr) alloy plates were used as negative control counterfaces and for damage simulation. Discrete scratches were created on the positive control CoCr plates using a diamond stylus with a spherical tip radius of 200 μm . The scratches on the positive controls (Figure 1) had a spacing of 1.5 mm

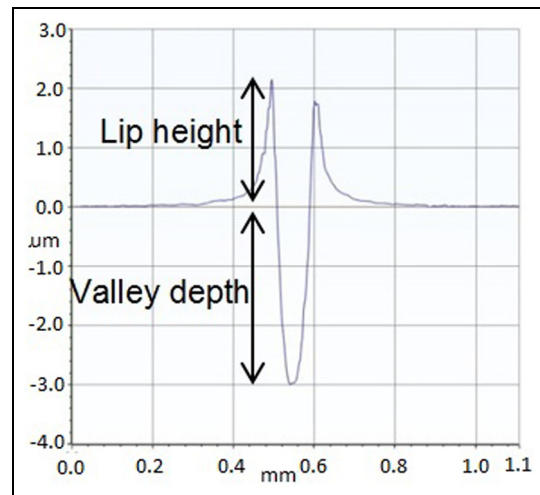


Figure 1. Positive control scratches damaged with a diamond stylus (mean lip height 2 μm), measurement taken with a Bruker NPFlex White Light Interferometer.

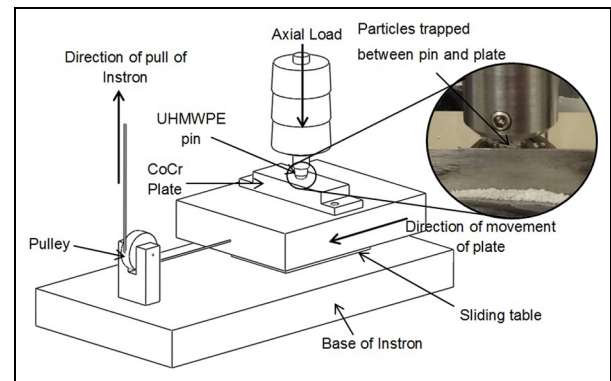


Figure 2. Schematic of the damage simulation rig with third-body particles trapped between UHMWPE pin and cobalt chrome plate (inset).

and an average lip height of 2 μm which is comparable in magnitude to scratches seen on explanted femoral heads⁹ and consistent with previous studies.¹⁰

Methods

Phase 1: third-body damage simulation. The protocol used was adapted from and validated against previous work by Minakawa.²⁴ Using a bespoke rig (Figure 2), third-body particles were trapped (in excess) between an UHMWPE pin and a highly polished CoCr plate. A load of 120 N was applied axially through the pin to trap the particles between the pin and plate and then using an Instron 3365 Materials testing machine (Instron, MA, USA), the plate was pulled beneath the pin at 8 mm/min to damage the surfaces. To create a worst case test, damage simulation was carried out without lubricant.

In each region of damage, the particles were passed over the plate five times in the same direction and five discrete regions of damage were generated. Following

damage simulation, the surface topography of the plates was analyzed using both two-dimensional (2D) contacting profilometry and white light interferometry. The surface roughness was determined using a PGI 800 contacting Form Talysurf profilometer (Taylor Hobson, Leicester, UK) with a $2\ \mu\text{m}$ conical tip stylus; the instrument had a z resolution of $3.2\ \text{nm}$ and a z repeatability of $0.12\ \text{nm}$. Least squares line form fitting was used to remove the background waviness of the surface and where appropriate filtering was used in line with ISO 4288:1998. The surface roughness parameters of interest were the mean surface roughness (R_a), the maximum profile height above the mean line averaged over appropriate sampling lengths (R_p), and the maximum valley depth (R_v). These parameters were chosen to give a measure of the overall surface damage caused by the different third-body particles as previous studies have demonstrated an exponential relationship between increasing R_p of scratches on a metal counterface and the wear of UHMWPE against the damaged surfaces.⁶ The mean lip height of the scratches and the density of scratches were determined from measurements taken by sampling the surface using a non-contacting Bruker NPFlex optical profiler (Bruker, MA, USA) with a $10\times$ lens which had an optical resolution of $0.9\ \mu\text{m}$ and a vertical resolution of $< 0.15\ \text{nm}$.³⁹ Images of the surface damage on the plates were captured at $63\times$ magnification using a PixelINK camera in combination with a Nikon SMZ800 stereomicroscope with illumination of the samples via an external light source. Four replicates were completed for each third-body material.

Phase 2: experimental wear simulation. A six-station multi-axial pin on plate reciprocating rig¹⁰ was used to determine the wear of UHMWPE articulating against the CoCr counterfaces damaged with different third-body particles. The damaged CoCr plate was secured in a lubricant containing bath which reciprocated at $1\ \text{Hz}$ with a stroke length of $\pm 20\ \text{mm}$. The pin was held in a pin holder which rotated ($\pm 20^\circ$) via a rack and pinion mechanism and was axially loaded with a constant load of $160\ \text{N}$ via a mass carrying cantilever mechanism to give a nominal contact pressure of $8.1\ \text{MPa}$ (Figure 3); wear simulation was carried out perpendicular to the direction of the damage simulation.

Wear simulation was performed at room temperature and lubricated with 25% (v/v) bovine serum supplemented with 0.03% sodium azide to retard bacterial growth to give a final protein concentration of approximately $15\ \text{g/L}$. Throughout the test, the level of the lubricant was maintained above the bearing surfaces.

The wear of the UHMWPE pins was determined by their loss in mass by gravimetric analysis. Prior to weighing, the pins were cleaned in 70% propan-2-ol in an ultrasonic bath and allowed to stabilise for 48 h in a temperature and humidity controlled environment. Measurements were taken before the wear test to set a datum, after 115,000 cycles which equates to 6 weeks in

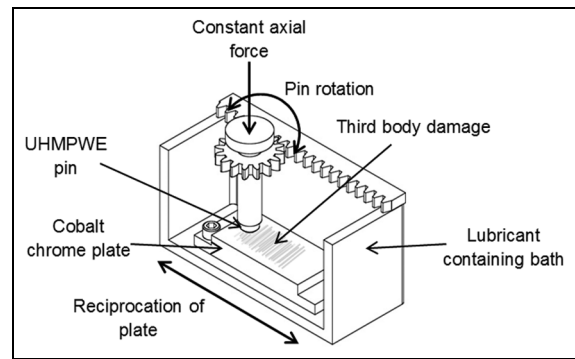


Figure 3. Section view of the lubricant containing bath used in the pin on plate wear test.

vivo based on 1 million cycles (MC) per year⁴⁰ and the duration the BVFs remain in the body before resorption and after 500,000 cycles equivalent to 6 months in vivo for the average patient with a moderate activity level. However, there is a wide variation in the activity levels between patients, and as the demands and demographics of patients change, it is likely that younger, more active patients⁴¹ will take a number of steps approaching 2 million.⁴² Unloaded soak controls were maintained in the same lubricant as used for testing. Gravimetric measurements were taken using an AT21 digital microbalance (Mettler Toledo Inc, OH, USA) with a readability of $1\ \mu\text{g}$ and a reproducibility of $2\ \mu\text{g}$. Each pin was weighed until five consecutive measurements were achieved in a range of $\pm 5\ \mu\text{g}$. The weight loss of the pins was converted to a volume loss (V) using the soak controls to compensate for moisture uptake and a density of $0.934\ \text{mg/mm}^3$ for GUR 1020 UHMWPE.⁴³ The wear factor (k) was calculated using the sliding distance for the test (X) and the applied load (P) as shown in equation (1).⁴⁴

$$k = \frac{V}{PX} \quad (1)$$

The wear of UHMWPE pins against plates damaged with third-body particles was compared to the wear against the highly polished ($R_a < 0.01\ \mu\text{m}$) negative control CoCr plates and positive control plates scratched with a diamond stylus.

Following wear simulation, surface topography measurements were repeated and the mean values with 95% confidence limits calculated. Statistical analysis was carried out using one-way analysis of variance (ANOVA) with Minitab 17⁴⁵ followed by a Tukey's post hoc test. Data were considered significant for $p < 0.05$.

The data associated with this article are openly available from the University of Leeds Data Repository.⁴⁶

Results

Phase 1: third-body damage simulation

Following damage simulation with PMMA and MGCS, scratches were evident on the surface of the

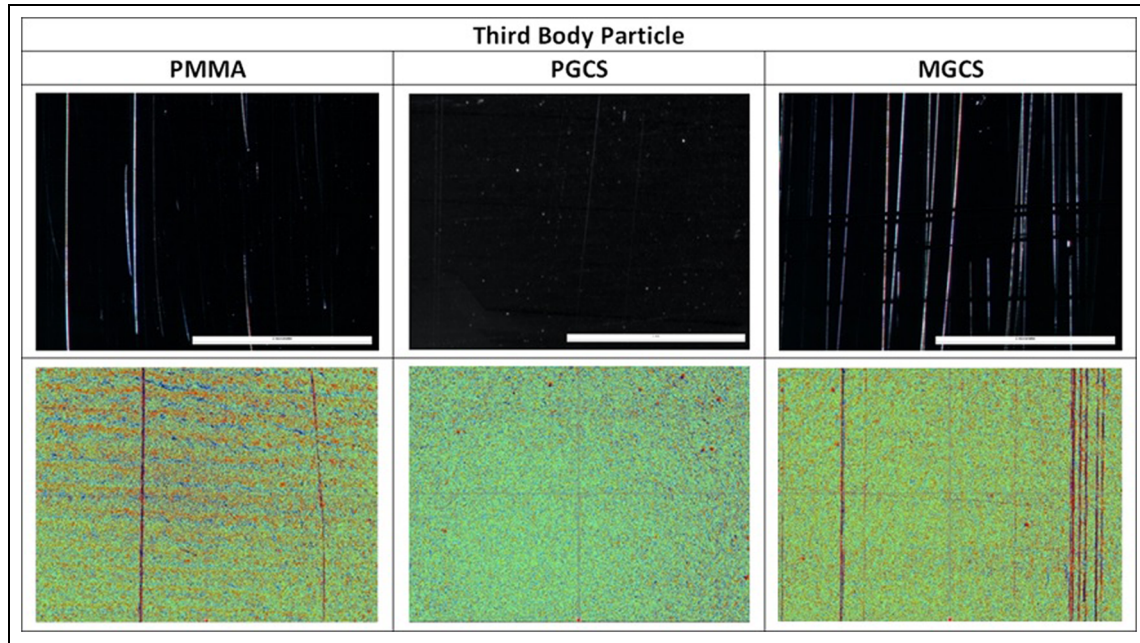


Figure 4. Images of the surface of the cobalt chrome plates at the conclusion of the study. Top: stereomicroscopy images (Nikon SMZ800 stereomicroscope) $63\times$ magnification, scale bar represents 1 mm. Bottom: white light interferometry measurements (Bruker NPFlex) $10\times$ magnification with $2.5\times$ multiplier, analysed with a robust Gaussian Filter, long wave cut-off of 0.04 mm and cylinder and tilt form removal.

Table 3. Analysis of scratches on the cobalt chrome plates following third-body damage simulation using the Bruker NPFlex White Light Interferometer (mean \pm 95% CL) analysed with a robust Gaussian Filter, long wave cut-off of 0.04 mm and cylinder and tilt form removal.

Scratching material	Number of scratches per mm	Mean lip height (mm)	Mean valley depth (mm)
PMMA	0.185 ± 0.208	0.028 ± 0.051	0.017 ± 0.031
PGCS	0	0	0
MGCS	1.615 ± 1.006	0.036 ± 0.019	0.016 ± 0.007

PGCS: pharmaceutical grade of calcium sulfate; MGCS: medical grade calcium sulfate; PMMA: polymethyl methacrylate.

cobalt chrome counterfaces as shown in the stereomicroscope images and white light interferometry measurements in Figure 4; no scratches were observed on the plates damaged with PGCS. The number of scratches and their mean lip height were analysed from the white light interferometry measurements, as shown in Table 3. There were no measurable scratches on the surface of the plates damaged with PGCS, the plates damaged with MGCS had 1.62 scratches per mm which was significantly ($p < 0.05$) higher than the number of scratches caused by PMMA. The scratches caused by MGCS had a mean lip height ($0.04 \pm 0.02 \mu\text{m}$) which was similar to those caused by PMMA ($0.03 \pm 0.05 \mu\text{m}$).

Prior to damage simulation, the mean surface roughness (R_a) of the plates was $< 0.01 \mu\text{m}$; following third-body damage simulation, the surface topography of the plates was measured using a contacting Form Talysurf in terms of R_a , R_p , and R_v as shown in Table 4. The mean surface roughness (R_a) of all the plates damaged with third-body particles was similar ($p > 0.05$), and there was no significant difference in the R_v or R_p of the

plates following third-body damage. The roughness data shown in Table 4 are filtered as per the ISO standard⁴⁷ to remove the background waviness, but there was a concern that in this case, the filtering led to an underestimation of the surface topography. The primary unfiltered data for the plates damaged with third-body particles are also shown in Table 4 and follow a similar trend to the analysis of the scratches with the white light interferometer, but there was no significant difference in P_p between the plates damaged with different third-body particles.

Phase 2: experimental wear simulation

Following damage simulation, the wear of UHMWPE articulating against the damaged plates was determined in a six-station pin on plate reciprocating rig perpendicular to the direction of damage simulation. At the conclusion of the wear simulation, there were light scratches on the surface of the plates in the principal direction of sliding and a polished appearance on the articulating surface of the UHMWPE pins where the

Table 4. Mean ($\pm 95\%$ CL) surface roughness (R_a values) of cobalt chrome plates perpendicular to damage following the scratching protocol measured using a contacting Form Talysurf (form removal and a Gaussian filter with 0.8-mm upper cut-off was applied to filter the data). p values show mean primary analysis ($\pm 95\%$ CL) following damage simulation with least squares line form removal but no filtering.

Scratching material	R_a (μm)	R_p (μm)	R_v (μm)	P_a (μm)	P_p (μm)	P_v (μm)
Negative control	0.005 ± 0.004	0.022 ± 0.018	0.016 ± 0.011			
Positive control	0.219 ± 0.010	1.360 ± 0.146	1.671 ± 0.097	0.243 ± 0.040	2.487 ± 0.244	3.169 ± 0.199
PMMA	0.006 ± 0.003	0.027 ± 0.022	0.016 ± 0.005	0.075 ± 0.058	0.150 ± 0.100	0.227 ± 0.159
PGCS	0.004 ± 0.001	0.023 ± 0.015	0.011 ± 0.003	0.057 ± 0.054	0.142 ± 0.095	0.178 ± 0.183
MGCS	0.006 ± 0.005	0.035 ± 0.029	0.018 ± 0.012	0.081 ± 0.089	0.213 ± 0.117	0.282 ± 0.315

PGCS: pharmaceutical grade calcium sulfate; MGCS: medical grade calcium sulfate; PMMA: polymethyl methacrylate.

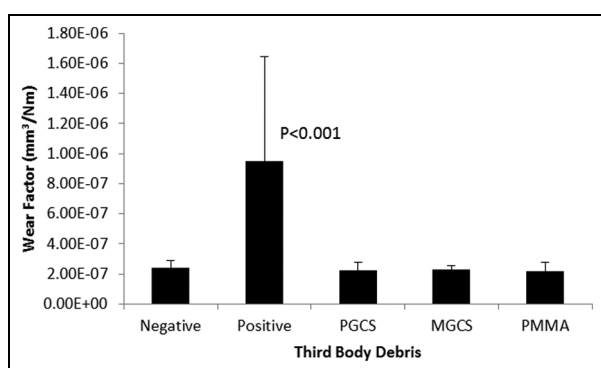


Figure 5. Mean wear factor ($\pm 95\%$ CL) of UHMWPE pins after 500,000 cycles of wear simulation. PGCS: pharmaceutical grade calcium sulfate; MGCS: medical grade calcium sulfate; PMMA: polymethyl methacrylate.

machining marks had been removed. Figure 5 shows the mean wear factor of the UHMWPE pins articulating against the control plates and those damaged with different third-body particles after 500,000 cycles of wear testing. Statistical analysis by one-way ANOVA showed a significant ($p < 0.001$) difference in the wear of the UHMWPE pins against the different counterfaces although post hoc analysis showed the wear to be similar against the plates damaged with third-body particles and the negative controls and significantly higher against the positive control plates.

Discussion

The approach used in this study was based on a previous methodology described by Minakawa,²⁴ which separated damage simulation and wear testing into two phases in a simple geometry pin on plate configuration. Pin on plate tests cannot replicate all the tribological variations found in a knee replacement but allow a single tribological variable, in this case the influence of surface damage on wear of UHMWPE to be isolated.⁶ In the first phase, damage simulation was carried out using different clinically relevant third-body particles to generate damage more representative of that seen in vivo.⁴ The high conformity of the flat on flat surfaces reduced the potential for the particles to migrate away

from the contact site.¹⁸ In the second phase, wear tests were carried out against the damaged surfaces. It is accepted practice to create surface damage and then to carry out wear testing,^{3,5,10} and by adopting this approach, both the surface topography of the cobalt chrome counterfaces and the wear of UHMWPE pins against the damaged surfaces were assessed.

Phase I: third-body damage simulation

There were no measurable scratches on the surface of the cobalt chrome plates damaged with PGCS, the damage created was below the resolution of the objective lens used (vertical resolution < 0.15 nm, lateral resolution $0.9 \mu\text{m}$);³⁹ MGCS caused scratches of the highest density and lip height of the third-body particles studied. The relative differences in the MGCS and PGCS materials have been discussed in literature.⁴⁸ MGCS is manufactured from the purification of naturally sourced gypsum with a typical purity in excess of 98% due to impurities such as calcium carbonate, magnesium carbonate, and “aggregate.”³⁷ PGCS is manufactured via a completely synthetic route and as such has a uniform crystalline structure which does not contain the potential for these impurities.³⁴ As the only difference between these two materials is the level of impurities as a result of the routes of manufacture, it is postulated that the presence of impurities in the calcium sulfate have an influence on the damage to the cobalt chrome surfaces. Following damage simulation with PMMA bone cement, scratches were visible on the surface of the plates. Several previous studies have investigated third-body damage with particles of PMMA bone cement of varying composition and have shown that during polymerization, the radiopacifiers in the cement agglomerate giving large, abrasive clusters which can damage metal counterfaces. The most commonly used radiopacifier particles in bone cement are zirconium dioxide and barium sulfate, and studies have shown zirconium dioxide to have a more detrimental effect on metallic counterfaces.^{8,18,21,49} The GMV bone cement used in this study contained barium sulfate; however, the magnitude of the surface damage caused by PMMA was lower than that caused by MGCS. A particle size range of 500–1000 μm diameter was used

for PMMA bone cement which is consistent with previous experimental wear simulation studies,²⁰ and observations of the size of bone cement particles present in the joint following lavage have shown the presence of particles up to 1 mm diameter.⁵⁰ While smaller diameter cement particles (< 100 μm) are frequently identified embedded in the polyethylene of retrieved knee replacements and surrounding tissue, it is particles of a larger diameter (~300 μm diameter) which are considered to cause more severe damage to the surfaces.⁵¹ The size of the indentations observed in retrieved UHMWPE tibial components of total knee replacements thought to be caused by particles of bone cement suggests that large cement particles may also become entrapped between the articulating surfaces, which break up during the loading and motion of the implant⁵² giving rise to smaller embedded PMMA particles in the UHMWPE.^{7,53,54}

It was noted that the different third-body materials behaved differently when loaded between two surfaces. When trapped between the pin and plate, the brittle calcium sulfate BVFs became a fine powder. The PMMA, however, maintained its particulate shape when trapped between an UHMWPE pin and a cobalt chrome plate and the particles were embedded into the pin. Particles of PMMA bone cement have been observed in UHMWPE acetabular cups of retrieved hip replacements⁵⁵ and the tibial components of retrieved total knee replacements.^{7,56,57} The resorbable nature of the BVFs⁵⁸ means that if they were to become trapped between the articulating surfaces of an implant, then over time, they would degrade so the duration the particles would be present in the joint would be relatively short, limiting damage to components. The inert and non-resorbable nature of trapped PMMA particles, however, means that while the magnitude of the damage they caused to the cobalt chrome counterfaces in this study was lower than that caused by MGCS, there is the potential for the embedded PMMA particles to cause continued roughening of the femoral component. As the roughness of the metal counterface has a strong influence on the wear rate of the UHMWPE component, increased abrasion of the UHMWPE will increase the generation of wear debris increasing the potential for osteolysis⁵⁹ and aseptic loosening which will ultimately reduce the life span of the implant.

Phase 2: experimental wear simulation

Against smooth negative control cobalt chrome plates, the wear of the UHMWPE pins was similar to studies carried out under similar kinematic conditions.⁶⁰ Previous studies have shown damage to the metal counterface resulting in an increased R_a to accelerate wear;⁶¹ however, a non-linear relationship between R_a , R_p , or lip height and wear has been exhibited, so that below a critical lip height, wear rate is similar to negative controls; Minakawa et al.⁶ described an

exponential relationship between R_p and wear factor showing when the R_p was < 0.5 μm , the wear was similar to highly polished controls, but an $R_p > 0.5 \mu\text{m}$ caused a dramatic increase in wear. A non-linear relationship between lip height and wear of non-crosslinked polyethylene was further demonstrated by Galvin et al.¹⁰ It was hypothesised that the third-body materials that caused surface damage with the highest lip heights would have the strongest influence on the rate of wear of UHMWPE. However, in this study, the damage caused by the third-body particles did not have lip heights of sufficient magnitude to increase the wear of UHMWPE above that of the negative controls. The wear was only significantly increased against positive control plates with a 2 μm lip height.

Conclusion

Third-body particles originating from PMMA bone cement and calcium sulfate BVFs can damage highly polished cobalt chrome counterfaces, and BVFs of similar composition can cause varying magnitudes of surface damage. Experimental wear simulation using a six-station pin on plate reciprocating rig against the damaged surfaces showed a similar rate of wear for UHMWPE pins articulating against negative (highly polished) plates and plates damaged with third-body particles and the wear rate was only increased in the positive control plates scratched with a diamond stylus (2 μm lip height). This study suggests that if calcium sulfate BVFs are used close to the articulating surfaces of total joint replacements, the purity of the calcium sulfate used may influence the magnitude of the surface damage. However, long-term wear tests of arthroplasty components should be carried out to determine whether the surface damage to cobalt chrome counterfaces caused by calcium sulfate BVFs influences UHMWPE wear volumes and ultimately the life span of total joint replacements.

Declaration of conflicting interests

The author(s) declared the following potential conflicts of interest with respect to the research, authorship, and/or publication of this article: Sean Aiken and John Cooper are paid employees of Biocomposites Ltd.

Funding

The author(s) disclosed receipt of the following financial support for the research, authorship, and/or publication of this article: This study was supported by Biocomposites Ltd which provided the bone void fillers and funding for the study.

References

1. National Joint Registry for England, Wales, and Northern Ireland. *11th annual report*. Hemel Hempstead: NJR Centre, 2014.

2. Fisher J, Jennings L, Galvin A, et al. 2009 Knee Society Presidential Guest Lecture: polyethylene wear in total knees. *Clin Orthop Relat Res* 2010; 468(1): 12–18.
3. Fisher J, Firkins P, Reeves EA, et al. The influence of scratches to metallic counterfaces on the wear of ultra-high molecular weight polyethylene. *Proc I MechE, Part H: J Engineering in Medicine* 1995; 209(4): 263–264.
4. McNie CM, Barton DC, Ingham E, et al. The prediction of polyethylene wear rate and debris morphology produced by microscopic asperities on femoral heads. *J Mater Sci Mater Med* 2000; 11(3): 163–174.
5. Barbour PSM, Stone MH and Fisher J. A hip joint simulator study using new and physiologically scratched femoral heads with ultra-high molecular weight polyethylene acetabular cups. *Proc I MechE, Part H: J Engineering in Medicine* 2000; 214(6): 569–576.
6. Minakawa H, Stone MH, Wroblewski BM, et al. Quantification of third-body damage and its effect on UHMWPE wear with different types of femoral head. *J Bone Joint Surg Br* 1998; 80-B(5): 894–899.
7. Jones VC, Williams IR, Auger DD, et al. Quantification of third body damage to the tibial counterface in mobile bearing knees. *Proc I MechE, Part H: J Engineering in Medicine* 2001; 215(2): 171–179.
8. Isaac GH, Atkinson JR, Dowson D, et al. The causes of femoral head roughening in explanted Charnley hip prostheses. *Eng Med* 1987; 16(3): 167–173.
9. Endo M, Tipper JL, Barton DC, et al. Comparison of wear, wear debris and functional biological activity of moderately crosslinked and non-crosslinked polyethylenes in hip prostheses. *Proc I MechE, Part H: J Engineering in Medicine* 2002; 216(2): 111–122.
10. Galvin A, Kang L, Tipper J, et al. Wear of crosslinked polyethylene under different tribological conditions. *J Mater Sci Mater Med* 2006; 17(3): 235–243.
11. Ries MD, Salehi A, Widding K, et al. Polyethylene wear performance of oxidized zirconium and cobalt-chromium knee components under abrasive conditions. *J Bone Joint Surg Am* 2002; 84(Suppl. 2): S129–S135.
12. DesJardins JD, Burnikel B and LaBerge M. UHMWPE wear against roughened oxidized zirconium and CoCr femoral knee components during force-controlled simulation. *Wear* 2008; 264(3–4): 245–256.
13. Wang A, Polineni VK, Stark C, et al. Effect of femoral head surface roughness on the wear of ultrahigh molecular weight polyethylene acetabular cups. *J Arthroplasty* 1998; 13(6): 615–620.
14. McKellop H, Shen F-W, DiMaio W, et al. Wear of gamma-crosslinked polyethylene acetabular cups against roughened femoral balls. *Clin Orthop Relat Res* 1999; 369: 73–82.
15. Bowsher JG and Shelton JC. A hip simulator study of the influence of patient activity level on the wear of cross-linked polyethylene under smooth and roughened femoral conditions. *Wear* 2001; 250(1–12): 167–179.
16. Glennon LP, Baer TE, Martin JA, et al. Sliding direction dependence of polyethylene wear for metal counterface traverse of severe scratches. *J Biomech Eng* 2008; 130(5): 051006.
17. Wang A and Essner A. Three-body wear of UHMWPE acetabular cups by PMMA particles against CoCr, alumina and zirconia heads in a hip joint simulator. *Wear* 2001; 250(1–12): 212–216.
18. Caravia L, Dowson D, Fisher J, et al. The influence of bone and bone cement debris on counterface roughness in sliding wear tests of ultra-high molecular weight polyethylene on stainless steel. *Proc I MechE, Part H: J Engineering in Medicine* 1990; 204(1): 65–70.
19. Davidson JA, Poggie RA and Mishra AK. Abrasive wear of ceramic, metal, and UHMWPE bearing surfaces from third-body bone, PMMA bone cement, and titanium debris. *Biomed Mater Eng* 1994; 4(3): 213–229.
20. Schroeder C, Grupp T, Fritz B, et al. The influence of third-body particles on wear rate in unicondylar knee arthroplasty: a wear simulator study with bone and cement debris. *J Mater Sci Mater Med* 2013; 24(5): 1319–1325.
21. Cooper JR, Dowson D, Fisher J, et al. Ceramic bearing surfaces in total artificial joints: resistance to third body wear damage from bone cement particles. *J Med Eng Technol* 1991; 15(2): 63–67.
22. Poggie RA, Mishra AK and Davidson JA. Three-body abrasive wear behaviour of orthopaedic implant bearing surfaces from titanium debris. *J Mater Sci Mater Med* 1994; 5(6–7): 387–392.
23. Bragdon CR, Jasty M, Muratoglu OK, et al. Third-body wear of highly cross-linked polyethylene in a hip simulator. *J Arthroplasty* 2003; 18(5): 553–561.
24. Minakawa H. *Quantification and simulation of third body damage to femoral heads and its effect on polyethylene wear in artificial hip joints*. Leeds: Department of Mechanical Engineering, University of Leeds, 1998.
25. Heuberger R, Wahl P, Kreig J, et al. Low *in vitro* third-body wear on total hip prostheses induced by calcium sulphate used for local antibiotic therapy. *Eur Cell Mat* 2014; 28: 246–257.
26. Chesney D, Sales J, Elton R, et al. Infection after knee arthroplasty: a prospective study of 1509 cases. *J Arthroplasty* 2008; 23(3): 355–359.
27. Jämsen E, Varonen M, Huhtala H, et al. Incidence of prosthetic joint infections after primary knee arthroplasty. *J Arthroplasty* 2010; 25(1): 87–92.
28. Moran E, Byren I and Atkins BL. The diagnosis and management of prosthetic joint infections. *J Antimicrob Chemother* 2010; 65(Suppl. 3): iii45–iii54.
29. Kalore NV, Gioe TJ and Singh JA. Diagnosis and management of infected total knee arthroplasty. *Open Orthop* 2011; 5: 86–91.
30. Kanellakopoulou K and Giamarellos-Bourboulis E. Carrier systems for the local delivery of antibiotics in bone infections. *Drugs* 2000; 59(6): 1223–1232.
31. Kelly CM, Wilkins RM, Gitelis S, et al. The use of a surgical grade calcium sulfate as a bone graft substitute: results of a multicenter trial. *Clin Orthop Relat Res* 2001; 382: 42–50.
32. Pietrzak WS and Ronk R. Calcium sulfate bone void filler: a review and a look ahead. *J Craniofac Surg* 2000; 11(4): 327–333.
33. Maale GE and Casas-Ganem JE. The use of antibiotic loaded synthesized calcium sulfate pellets in the one stage treatment for Osteomyelitis. In: *Annual open scientific meeting of the Musculoskeletal Infection Society*, San Diego, CA, 7–8 August 2009, pp.7–8.
34. McPherson E, Dipane M and Sherif S. Dissolvable antibiotic beads in treatment of periprosthetic joint infection and revision arthroplasty—the use of synthetically pure

- calcium sulfate (Stimulan) impregnated with vancomycin and tobramycin. *Reconstr Rev* 2013; 3(1): 32–43.
35. Winkler H. Rationale for one stage exchange of infected hip replacement using uncemented implants and antibiotic impregnated bone graft. *Int J Med Sci* 2009; 6(5): 247–252.
 36. Wenke JC, Owens BD, Svoboda SJ, et al. Effectiveness of commercially-available antibiotic-impregnated implants. *J Bone Joint Surg Br* 2006; 88-B(8): 1102–1104.
 37. <http://documents.wright.com/Document/Get/010662>, 2014.
 38. Fisher J, McEwen HM, Tipper JL, et al. Wear, debris, and biologic activity of cross-linked polyethylene in the knee: benefits and potential concerns. *Clin Orthop Relat Res* 2004; 428: 114–119.
 39. Bruker. NPFLEX objectives chart, 2012, <http://bruker-nano.actonsoftware.com/acton/attachment/9063/f-01d0/0/-/-/-/-/NPFLEX%20Objectives%20Chart%20Data-sheet%20-%20DS555-RevA0.pdf>
 40. Schmalzried TP, Szuszczewicz ES, Northfield MR, et al. Quantitative assessment of walking activity after total hip or knee replacement. *J Bone Joint Surg Am* 1998; 80(1): 54–59.
 41. Jennings LM, Al-Hajjar M, Brockett CL, et al. (iv) Enhancing the safety and reliability of joint replacement implants. *Orthop Trauma* 2012; 26(4): 246–252.
 42. Silva M, Shepherd EF, Jackson WO, et al. Average patient walking activity approaches 2 million cycles per year: pedometers under-record walking activity. *J Arthroplasty* 2002; 17(6): 693–697.
 43. McEwen HMJ, Fisher J, Goldsmith AAJ, et al. Wear of fixed bearing and rotating platform mobile bearing knees subjected to high levels of internal and external tibial rotation. *J Mater Sci Mater Med* 2001; 12(10–12): 1049–1052.
 44. Fisher J. Wear of ultra high molecular weight polyethylene in total artificial joints. *Curr Orthop* 1994; 8(3): 164–169.
 45. Minitab, Inc. *Minitab 17 Statistical Software*. State College, PA: Minitab, Inc., 2010.
 46. Cowie RM and Jennings LM. Data associated with “Influence of Third Body Particles Originating from Bone Void Fillers on the Wear of Ultra High Molecular Weight Polyethylene” [dataset]. University of Leeds, 2016, <http://doi.org/10.5518/62>
 47. ISO 4288:1998. Geometric product specification (GPS). Surface texture—profile method: rules and procedures for the assessment of surface texture.
 48. Parker AC, Smith JK, Courtney HS, et al. Evaluation of two sources of calcium sulfate for a local drug delivery system: a pilot study. *Clin Orthop Relat Res* 2011; 469(11): 3008–3015.
 49. Manero JM, Gil FJ, Ginebra MP, et al. Wear behaviour of the pair Ti-6Al-4V-UHMWPE of acrylic bone cements containing different radiopaque agents. *J Biomater Appl* 2004; 18(4): 305–319.
 50. Niki Y, Matsumoto H, Otani T, et al. How Much sterile saline should be used for efficient lavage during total knee arthroplasty? Effects of pulse lavage irrigation on removal of bone and cement debris. *J Arthroplasty* 2007; 22(1): 95–99.
 51. McNie CM, Barton DC, Fisher J, et al. Modeling of damage to articulating surfaces by third body particles in total joint replacements. *J Mater Sci Mater Med* 2000; 11(9): 569–578.
 52. Trent PS and Walker PS. Wear and conformity in total knee replacement. *Wear* 1976; 36(2): 175–187.
 53. Wasielewski RC, Galante JO, Leighty RM, et al. Wear patterns on retrieved polyethylene tibial inserts and their relationship to technical considerations during total knee arthroplasty. *Clin Orthop Relat Res* 1994; 299: 31–43.
 54. Landy MM and Walker PS. Wear of ultra-high-molecular-weight polyethylene components of 90 retrieved knee prostheses. *J Arthroplasty* 1988; 3(Suppl.): S73–S85.
 55. Atkinson JR, Dowson D, Isaac GH, et al. Laboratory wear tests and clinical observations of the penetration of femoral heads into acetabular cups in total replacement hip joints: II: a microscopical study of the surfaces of Charnley polyethylene acetabular sockets. *Wear* 1985; 104(3): 217–224.
 56. Kelly NH, Fu RH, Wright TM, et al. Wear damage in mobile-bearing TKA is as severe as that in fixed-bearing TKA. *Clin Orthop Relat Res* 2011; 469(1): 123–130.
 57. Gabriel SM, Dennis DA, Honey MJ, et al. Polyethylene wear on the distal tibial insert surface in total knee arthroplasty. *Knee* 1998; 5(3): 221–228.
 58. Parikh SN. Bone graft substitutes: past, present, future. *J Postgrad Med* 2002; 48(2): 142–148.
 59. Tipper JL, Ingham E, Hailey JL, et al. Quantitative analysis of polyethylene wear debris, wear rate and head damage in retrieved Charnley hip prostheses. *J Mater Sci Mater Med* 2000; 11(2): 117–124.
 60. Kang L, Galvin AL, Brown TD, et al. Quantification of the effect of cross-shear on the wear of conventional and highly cross-linked UHMWPE. *J Biomech Eng* 2008; 41(2): 340–346.
 61. Lancaster JG, Dowson D, Isaac GH, et al. The wear of ultra-high molecular weight polyethylene sliding on metallic and ceramic counterfaces representative of current femoral surfaces in joint replacement. *Proc I MechE, Part H: J Engineering in Medicine* 1997; 211(1): 17–24.